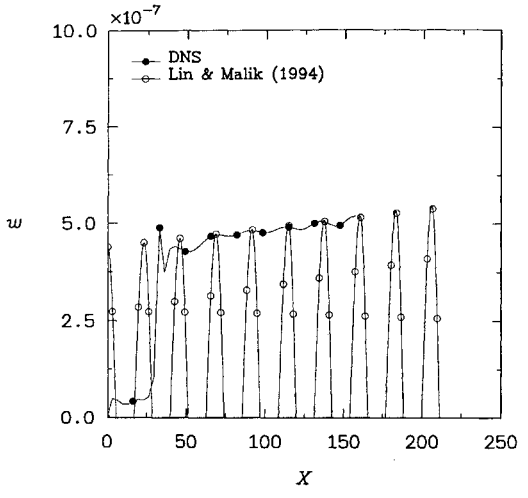

Fig. 3 Asymmetric disturbance (A1) growth compared with theory for three-dimensional attachment-line basic flow for $R = 7 \times 10^2$ and $\omega = 0.1017$.

inevitable in this three-dimensional flow. To make this comparison, the results for the simulation are averaged over the flow-acceleration stations: $z = 0$ and $z = \pm 6$. These stations were selected because, as Joslin[10] shows, the streamlines very near the attachment line are essentially aligned with the two-dimensional attachment-line flow. The $z = \pm 6$ stations permit a cancellation of any opposing flow-acceleration effects.

Concluding Remarks

In this study, results are presented for the spatial DNS of three-dimensional symmetric and asymmetric disturbances that propagate along the attachment line of swept Hiemenz flow. The comparison between the DNS results and the theoretical results demonstrate that both symmetric and asymmetric modes are present in the attachment-line flow and that the theory adequately predicts these modes and the relative dominance of each mode.

Although the connection between the linear instability $R_\theta \simeq 2.45 \times 10^2$ and the turbulent contamination $R_\theta \simeq 1 \times 10^2$ regions was not definitively explained, it is clear that a wealth of instabilities can be present within this three-dimensional flowfield and that some combination of these modes interacting in a nonlinear manner will likely resolve this region of study.

Acknowledgment

The author wishes to express his gratitude to R.-S. Lin, High Technology Corporation, for providing the initial disturbance information for the simulations.

References

[1]Cumpsty, N. A., and Head, M. R., "The Calculation of the Three-Dimensional Turbulent Boundary Layer. Part III. Comparison of Attachment-Line Calculations with Experiment," *Aeronautical Quarterly*, Vol. 20, May 1969, pp. 99–113.

[2]Pfenninger, W., and Bacon, J. W., Jr., "Amplified Laminar Boundary-Layer Oscillations and Transition at the Front Attachment Line of a 45 Degree Swept Flat-Nosed Wing With and Without Boundary-Layer Suction," *Viscous Drag Reduction*, edited by C. S. Wells, Plenum, New York, 1969, pp. 85–105.

[3]Poll, D. I. A., "Transition in the Infinite Swept Attachment Line Boundary Layer," *Aeronautical Quarterly*, Vol. 30, Nov. 1979, pp. 607–628.

[4]Poll, D. I. A., "Three-Dimensional Boundary Layer Transition via the Mechanisms of Attachment-Line Contamination and Crossflow Stability," *Laminar-Turbulent Transition*, edited by R. Eppler and H. Fasel, Springer, Stuttgart, Germany, 1980, pp. 253–262.

[5]Hall, P., Malik, M. R., and Poll, D. I. A., "On the Stability of an Infinite Swept Attachment Line Boundary Layer," *Proceedings of the Royal Society of London, Series A: Mathematical and Physical Science*, Vol. 395, Oct. 1984, pp. 229–245.

[6]Spalart, P. R., "Direct Numerical Study of Leading-Edge Contamination," AGARD, CP-438, 1989, pp. 5.1–5.13.

[7]Theofilis, V., "Numerical Experiments on the Stability of Leading Edge Boundary Layer Flow: A Two-Dimensional Linear Study," *International Journal for Numerical Methods in Fluids*, Vol. 16, Jan. 1993, pp. 153–170.

[8]Jiménez, J., Martel, C., Agüí, J. C., and Zufiria, J. A., "Direct Numerical Simulation of Transition in the Incompressible Leading Edge Boundary Layer," *ETSIA/MF-903*, Universidad Politecnica Madrid, Spain, 1990.

[9]Joslin, R. D., "Direct Simulation of Evolution and Control of Nonlinear Instabilities in Attachment-Line Boundary Layers," AIAA Paper 94-0826, Jan. 1994.

[10]Joslin, R. D., "Direct Simulation of Evolution and Control of Three-Dimensional Instabilities in Attachment-Line Boundary Layers," *Journal of Fluid Mechanics*, Vol. 291, May 1995, pp. 369–392.

[11]Pfenninger, W., "Flow Phenomena at the Leading Edge of Swept Wings," *Recent Developments in Boundary Layer Research*, AGARD 97, May 1965.

[12]Gregory, N., and Love, E. M., "Laminar Flow on a Swept Leading Edge," National Physical Lab., Final Progress Rept., NPL Aero. Memo., Vol. 26, Oct. 1965.

[13]Gaster, M., "On the Flow Along Swept Leading Edges," *Aeronautical Quarterly*, Vol. 18, May 1967, pp. 165–184.

[14]Poll, D. I. A., "Some Observations of the Transition Process on the Windward Face of a Long Yawed Cylinder," *Journal of Fluid Mechanics*, Vol. 150, Jan. 1985, pp. 329–356.

[15]Hall, P., and Malik, M. R., "On the Instability of a Three-Dimensional Attachment-Line Boundary Layer: Weakly Nonlinear Theory and a Numerical Simulation," *Journal of Fluid Mechanics*, Vol. 163, Feb. 1986, pp. 257–282.

[16]Lin, R.-S., and Malik, M. R., "The Stability of Incompressible Attachment-Line Boundary Layers—A 2D-Eigenvalue Approach," AIAA Paper 94-2372, June 1994.

[17]Lin, R.-S., and Malik, M. R., "Stability and Transition in Compressible Attachment-Line Boundary-Layer Flow," Aerotech '95, Society of Automotive Engineers, SAE Paper 952041, Los Angeles, CA, Sept. 1995.

[18]Fedorov, S., personal communication, Moscow Inst. of Physics and Technology, Zhukovsky, Russia, 1995.

Transition Detection with Deposited Hot Films in Cryogenic Tunnels

Ehud Gartenberg*
Old Dominion University, Norfolk, Virginia 23529-0247
and
Michael A. Scott† and Scott D. Martinson‡
NASA Langley Research Center, Hampton, Virginia 23681-0001

Introduction

CRYOGENIC wind tunnels are high Reynolds number facilities, capable of producing on models the Mach–Reynolds numbers combinations occurring on large transport airplanes in flight. These are subsonic and transonic tunnels in which liquid nitrogen is continuously injected into the stream and gas is vented to keep the pressure and temperature values at the desired test condition. The temperature can be varied between ambient and 120 K, while the pressure can be varied according to the tunnel's design. Under typical test conditions, the unit Reynolds number is 30 to 40 times higher than in flight, and about 4 times higher than in conventional tunnels operating at identical pressures. The capability to detect boundary-layer

Received June 30, 1995; revision received July 16, 1996; accepted for publication July 22, 1996; also published in *AIAA Journal on Disc*, Volume 2, Number 1.

*Research Associate Professor, Department of Mechanical Engineering. Associate Fellow AIAA.
†Aerospace Technologist, Aerodynamic Measurement Branch, MS 234.
‡Aerospace Technologist, Acoustical, Optical, and Chemical Measurement Branch, MS 236.

transition in these tunnels is required for studies of Reynolds number effects, wind tunnel to flight correlations, and laminar-flow testing. Whereas the extent of the laminar flow and the transition mechanism can be efficiently identified with infrared (IR) imaging,[1] an array of chordwise deposited hot films can provide temporal/spectral information on the boundary-layer instability at multiple locations. The information from IR imaging and the deposited films complement each other; moreover, the dielectric substrate of the films also provides the radiation and insulation characteristics required for the IR imaging of the surface.

The very thin boundary layer generated by high unit Reynolds number flows imposes severe limitations on the thickness of the hot films, to avoid premature transition and additional drag caused by the interaction with the viscous sublayer of the turbulent regime. These requirements are critical for model testing, where the drag is determined globally from balance measurements. Allowable thicknesses for deposited hot films operated in high Reynolds number flows are illustrated through two closed-form examples. First, a slender cone at zero angle of attack is considered, the length of its laminar boundary layer being accepted as indicative of the wind tunnel's flow quality. In the transonic regime, the laminar boundary layer over a 10-deg cone undergoes transition around a Reynolds number of $Re = 4 \times 10^6$. Using Mangler's transformation,[2] the laminar boundary-layer thickness in this case is related to that over a flat plate by a factor of $1/\sqrt{3}$, i.e., $\delta = 2.887\sqrt{[x/(Re/m)]} = 2.887\sqrt{(Re)/(Re/m)}$. Following Goldstein,[3] the allowable height k of a single wire protuberance to avoid triggering transition is given by $ku^*/\nu = 7$, which for the cone under consideration yields $k = 9.23Re^{0.25}/(Re/m)$, where ν is the kinematic viscosity and the local friction velocity $u^* = \sqrt{(\tau/\rho)}$, where τ is the shearing stress and ρ is the density. Now, at typical transonic cryogenic conditions[4] of $Re = 200 \times 10^6$/m, the laminar boundary layer undergoes transition at 0.02 m from the apex, where $\delta = 29$ μm. At 0.01 m from the apex, halfway into the laminar regime, $\delta = 20$ μm, and therefore $k = 1.7$ μm. The second case refers to films that operate downstream of the transition zone, and may interact with the viscous sublayer of the turbulent boundary layer, shedding vorticity and increasing the drag of the body. For relatively planar surfaces with small pressure gradients, Schlichting[5] proposed a limiting criterion $k \leq 100/(Re/m)$, which for a typical cryogenic flow of $Re = 200 \times 10^6$/m yields $k = 0.5$ μm. These examples illustrate the need for films about 1 μm (10^{-6} m) thick. Similar considerations led Fancher[6] to propose the fabrication of microthin hot films and their leads by depositing the metals directly on the model's surface. The concept was developed over the years, and a number of fabrication alternatives were tried; however, its implementation faced considerable difficulties.[7-10] (Note that Fig. 11 of Ref. 10 displays the output of the only film out of 30 that survived the calibration at lower temperatures.) More recently, the fabrication and anemometry procedures were sufficiently refined, and the concept was finally proven at the lowest operational temperatures of cryogenic wind tunnels in several tests that lasted between one and two weeks each, with no loss of hot films.

Technological and Operational Considerations

The metal deposition on models is done in vacuum chambers following industrial practice for mirror finish coatings. During the deposition process, the pressure orifices of the model should be protected, to avoid clogging. The film thickness is determined from the frequency shift that the deposited metal causes to a quartz oscillator, which is placed in the deposition area. The technique has a resolution of 1 Å(10^{-10} m), whereas typical accumulation rates are of the order of 2–3 Å/s. (Reference 11 incorporates a brief discussion of this technique and a few references.) Experience indicates that three main factors affect the quality and longevity of the films: 1) the surface smoothness, 2) the firm adhesion of the deposited metal to its substrate, and 3) the ability of the substrate to match the thermal strain of the films. These factors are essential in preventing failure through thermal buckling, hot spots, and ultimately melting, mostly through effective thermal dissipation into the substrate. The current deposition technique is capable of producing films with a success rate of better than 90% and with excellent survival records in cryogenic flows. The films' spacing is determined by the width of the leads (on the order of millimeters), depending on the desired thickness and resistance. The hot films' control and data acquisition is based on constant temperature anemometry (CTA), which maintains the films at a constant resistance (within 1/10 Ω), corresponding to a designated temperature. The calibration is done in a cryo-oven chamber, where the instrumented model is cycled thermally, and resistance readings of individual films are taken over the range of interest. The ratio between the hot and cold resistance of a film is defined as the overheat ratio, which during wind-tunnel tests was set at 1.2, following pretesting in cryo chambers at ratios up to 1.6. It is essential to adjust the overheat ratio at each test condition, as the setting at one flow temperature results in a different value at another flow temperature. Neglecting this CTA aspect in cryogenic testing causes the electrical current through the hot films to increase significantly as the flow temperature decreases, and may cause their failure. In such cases, the broken films appear partially melted and lifted off the substrate, suggesting thermal buckling and hot spot formation. The failure is caused by the expansion of the hot film clamped between its relatively cold ends accompanied by a loosening of the adhesion to its substrate, which in turn denies the ability of dissipating some of the heat into the substrate.

Figure 1 shows a NASA SC(3)-0712 composite airfoil instrumented with deposited films. This model is fabricated from a metallic spar wrapped in fiberglass epoxy, with pressure tubes laid along slits cut spanwise in the spar. Orifices drilled through the transparent fiberglass-epoxy layers at the open ends of the tubes allow surface pressure measurements. This technique is cheaper and faster compared to the fabrication of metallic models of identical surface quality. In addition, composite models can be remade in case of surface degradation or fabrication undercut. With a roughness of 0.1 μm rms, this model has the best surface quality of all of the concepts tested. In this case, the metals were deposited through masks. The films' frequency response, as determined from standard square wave tests, is not uniform among the sensors, and it is currently limited to 8 kHz. Two other variants were also considered.[11] In the second case, an HSNLF(1)-0213 aluminum airfoil was covered with a layer of polyimide that was sprayed and cured successively to a cumulative thickness of 45 μm. The nickel and the copper were deposited over a wide area, the films and the leads being patterned by removing metal using photolithography. The surface roughness of the coating was 0.18-μm rms, which is smoother than the original metallic surface thanks to the filling of the metal's microscopic groves with polyimide. The thickness of the films was identical to the previous case. However, their frequency response was more uniform and considerably higher, about 45 kHz. The third case was an SC(3)-0712 steel airfoil with films photolithographed on a polyimide sheet, which was thereafter glued to the model using the vacuum bag technique. The polyimide sheet is 180 μm thick, and its roughness is directional, 0.25-μm rms in one direction and 0.50-μm rms in the perpendicular direction. In this case, the film's thickness was 0.25 μm, and the lead's thickness was augmented to 7.6 μm to allow a denser spacing. These films were the most robust of all of the types tested; furthermore, their frequency response was the most uniform, about 25 kHz.

The airfoil shown in Fig. 1 has two opposite hot-film arrays, one aligned chordwise and the other slanted 18 deg to the chord. Staggering of hot films is a known procedure to measure the development of laminar-boundary layer instability while avoiding streamline contamination from upstream sensors. To verify the adequacy of deposited films for laminar flow research, the output of the two hot-film arrays was compared; a typical sample of the time traces is shown in Fig. 2. The two blank slots represent malfunctioning channels traced to loose electrical connections. The measurements reproduced in this figure were taken at a low Reynolds number and at a negative angle of attack, which produces a favorable pressure gradient, thus stabilizing the laminar boundary layer over the forward region of the airfoil. The comparison between the output of the two arrays indicates that the boundary layer over the aligned films underwent transition both sooner and faster

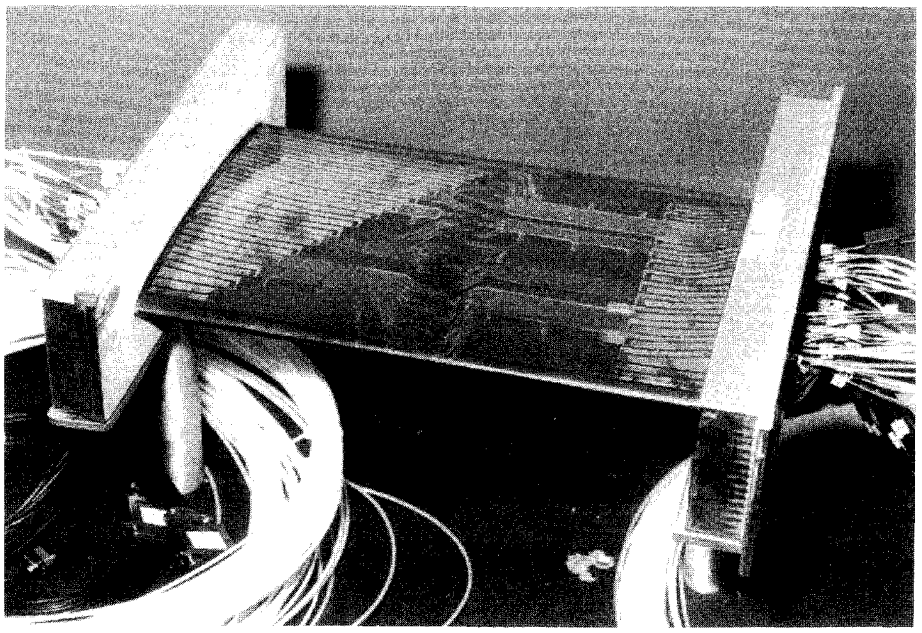

Fig. 1 SC(3)-0712 airfoil with 229-mm chord fiberglass-epoxy on steel spar with directly deposited hot films: surface roughness 0.1-μm rms, nickel hot films 0.25 μm thick, copper leads 1.0 μm thick, frequency response up to 8 kHz.

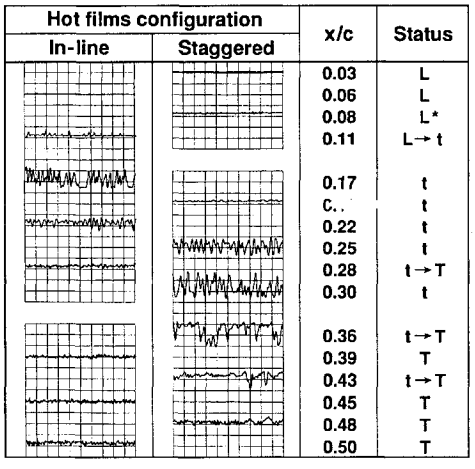

Fig. 2 Voltage time traces (ac component) from constant temperature anemometers and the microthin hot films deposited on the airfoil shown in Fig. 1: $T_t = 110$ K, $p_t = 1.24$ bar, $M = 0.2$, $\alpha = -4.8$ deg, $Re_c = 4.9 \times 10^6$, 1 ms/div, 500 mV/div. *L*, laminar; *t*, transitional; *T*, turbulent; and *, noisy channel.

compared with the undisturbed boundary layer measured with staggered films. The following factors, alone or combined, may have contributed to the accelerated transition indicated by the aligned films: 1) starting the array too close to the leading edge, 2) the inadequacy of the allowable thickness criterion for a single wire to be applied to an array of films, or 3) thermal contamination of the boundary layer from succeeding hot films. In any case, this result indicates the necessity to stagger even microthin deposited hot films.

In light of their recent successful operational record, we conclude that microthin deposited hot films can be considered operational over the entire temperature range of cryogenic wind tunnels, down to 100 K. Although of micronic thickness, deposited hot films should be staggered to avoid downstream measurement contamination. The dielectric substrate required for the operation of deposited hot films is compatible with the IR imaging method for transition detection,[12] thus allowing concomitant global mapping and local temporal measurements of the boundary-layer transition. As expected, it was observed that the frequency response increases with the thermal diffusivity of the substrate.

Acknowledgments

The first author was supported through NASA Task NAS1-18584-151. He expresses his gratitude to James E. Bartlett and Sang Q. Tran, both with the Microelectronics and Sensor Development Section at NASA Langley Research Center, for their sustained effort to develop the hot-films deposition technology.

References

[1]Gartenberg, E., "Milestones in Boundary-Layer Transition Research with Infrared Imaging," *Proceedings of Wind Tunnels and Wind Tunnels Test Techniques* (Southampton Univ.), Royal Aeronautical Society, London, 1992 (Paper No.10).

[2]Mangler, W., "Zusammenhang zwischen ebenen und rotationssymmetrischen Grenzschichten in kompressiblen Flussigkeiten," *Zeitschrift fur Angewandte Mathematik und Mechanik*, Vol. 28, 1948, pp. 97–103.

[3]Goldstein, S., "A Note on Roughness," Aeronautical Research Council Repts. and Memoranda 1763, London, 1936.

[4]Gartenberg, E., "A Concept for Transition Mapping on a 10°-Cone in the National Transonic Facility Using Flow-Pressure Variation," NASA CR-198209, Sept. 1995.

[5]Schlichting, H., *Boundary-Layer Theory*, 7th ed., McGraw–Hill, New York, 1979, p. 660.

[6]Fancher, M. F., "Aspects of Cryogenic Wind Tunnel Testing Technology at Douglas," AIAA Paper 82-0606, March 1982.

[7]Johnson, C. B., Carraway, D. L., Stainback, P. C., and Fancher, M. F., "A Transition Detection Study a Using Cryogenic Hot Film System in the Langley 0.3-Meter Transonic Cryogenic Tunnel," AIAA Paper 87-0049, Jan. 1987.

[8]Johnson, C. B., Carraway, D. L., Stainback, P. C., and Fancher, M. F., "Detecting Boundary-Layer Transition in Cold Environment," NASA Tech. Briefs, March 1990, p. 76.

[9]Johnson, C. B., Carraway, D. L., Hopson, P., Jr., and Tran, S. Q., "Status of a Specialized Boundary Layer Transition Detection System for the Use in the U.S. National Transonic Facility," *International Congress on Instrumentation in Aerospace Facilities*, Inst. of Electrical and Electronics Engineers, New York, 1987, pp. 141–155.

[10]Gartenberg, E., Johnson, W. G., Johnson, C. B., Carraway, D. L., and Wright, R. E., "Transition Detection Studies in the Cryogenic Environment," *Proceedings of the 8th Applied Aerodynamics Conference*, AIAA, Washington, DC, 1990, pp. 234–244.

[11]Gartenberg, E., "Development and Implementation of the First Set of Flow-Diagnostic Techniques for Cryogenic Wind Tunnels," AIAA Paper 96-2203, June 1996.

[12]Gartenberg, E., and Wright, R. E., "Boundary-Layer Transition Detection with Infrared Imaging Emphasizing Cryogenic Applications," *AIAA Journal*, Vol. 32, No. 9, 1994, pp. 1875–1882.